Cluster Dynamics Study of Neutron Irradiation Induced Defects in Fe-12.5at%Cr Alloy

4 authors, including:

Some of the authors of this publication are also working on these related projects:

Fatigue crack growth in aluminum alloys View project

Dispersion Strengthened Materials View project

Cluster Dynamics Study of Neutron Irradiation Induced Defects in Fe-12.5at%Cr Alloy

Aleksandr Gokhman [1, a], Andreas Ulbricht [2, b], Uwe Birkenheuer [2, c],

Frank Bergner [2, d]

[1] South Ukrainian National Pedagogical University (Ukraine)

[2] Research Center Dresden-Rossendorf (Germany)

[a]gokhman@paco.net, [b]A.Ulbricht@fzd.de, [c]u.birkenheuer@fzd.de, [d]f.bergner@fzd.de

Keywords: Cluster dynamics, neutron irradiation, chromium iron alloys, defects

Abstract. Cluster dynamics (CD) is used to study the evolution of the size distributions of vacancy clusters (VC), self-interstitial atom (SIA) clusters (SIAC) and Cr precipitates in neutron irradiated Fe-12.5at%Cr alloys at $T = 573\ K$ with irradiation doses up to 12 dpa and a flux of 140 ndpa/s. Transmission electron microscopy (TEM) and small angle neutron scattering (SANS) data on the defect structure of this material irradiated at doses of 0.6 and 1.5 dpa are used to calibrate the model. A saturation behavior was found by CD for the free vacancy and free SIA concentrations as well as for the number density of the SIAC and the volume fraction of the Cr precipitates for neutron exposures above 0.006 dpa. The CD simulations also indicate the presence of VC with radii less than 0.5 nm and a strong SIAC peak with a mean diameter of about 0.5 nm, both invisible in SANS and TEM experiments. A specific surface tension of about 0.028 J/m^2 between the α matrix and the Cr-rich α' precipitate was found as best fit value for reproducing the long-term Cr evolution in the irradiated Fe-12.5%Cr alloys observed by SANS.

Introduction

Ferritic-martensitic chromium steels are candidate structural materials for future generation nuclear reactors such as fusion or advanced high temperature reactors (Gen IV) or spallation sources, because of their remarkable resistance to swelling and of their adequate mechanical properties. In operation, these materials will be exposed to high neutron doses (up to about 100 dpa) and high temperatures. However, the formation of irradiation-induced defects and the possible degradation of the mechanical properties under these extreme conditions is not yet well understood. The investigation of neutron-irradiated binary Fe-Cr alloys will significantly contribute to the understanding of the behavior of more complex alloys. TEM (transmission electron microscopy) and SANS (small angle neutron scattering) data [1, 2] are related to the defect structure obtained by CD (cluster dynamics) simulation on irradiated Fe-12.5at%Cr model alloys for two different neutron doses.

For the purpose of predicting irradiation hardening it is necessary to know in detail the size distributions of vacancy clusters (VC) and self-interstitial atom clusters (SIAC) formed under irradiation at any neutron dose. The latter can be obtained by means of CD modeling.

Irradiation Conditions and Experimental Data

The irradiation conditions and experimental results described in [1, 2] are summarized below for the purpose of comparison with the CD simulations performed in this study. The material (average grain size 1 µm, pre-existing dislocation density 5.5×10^{13} m^{-2}) was neutron-irradiated in the Callisto rig (IPS2) in the Belgian reactor (BR2). An irradiation temperature T of 573 K and a neutron flux of about 9×10^{17} n/m^{2}s ($E > 1$ MeV) were maintained. This flux corresponds to a dose rate of about 140 ndpa/s. The neutron exposure covered the range from 0.6 to 1.5 dpa. TEM investigations reveal

the presence of dislocation loops of size 6 nm (in diameter) and a total loop density about 1.73×10^{21} m^{-3} for both irradiation conditions, 0.6 and 1.5 dpa. No voids were observed by TEM under these irradiation conditions. Irradiation-induced features with diameter of about 2 nm and volume fraction of (4.3 ± 0.4) % for both irradiation conditions and A-ratios (ratio of total and nuclear SANS intensity) of 2.07 ± 0.05 and 2.05 ± 0.05 for a dose of 0.6 and 1.5 dpa, respectively, have been found by SANS. These features were related to pure Cr precipitates in α-Fe as well as to α' particles dispersed in the α-Fe matrix. In [2] a decrease in the scattering cross-section of SANS with decreasing scattering vector, Q, was found, as is typical for the interference effects in concentrated alloys. The size distribution of the α' particles reported in [2], was obtained by the indirect transformation method applied to the fitted measured nuclear scattering cross sections. The range of the Q-values was restricted to values great than 1 nm^{-1} in the fit, where interference effect can be excluded.

Table 1. Material parameters of matrix defect system

Material parameters	pure iron [4]	present study
Vacancy formation energy E_f [eV]	1.60	1.60
Binding energy of a vacancy dimer E_{b2v} [eV]	0.608	0.608
Vacancy migration energy E_{mv} [eV]	~~0.85~~	0.88
Vacancy pre-exponential factor D_{vo} [m^2/s]	2.1×10^{-8}	2.1×10^{-8}
Interstitial formation energy E_{fi} [eV]	3.05	3.0
Binding energy of an interstitial dimer E_{b2i} [eV]	0.8	0.8
Interstitial migration energy E_{mi} [eV]	0.30	0.24
Interstitial pre-exponetnial factor D_{io} [m^2/s]	3.6×10^{-8}	4.8×10^{-8}
Recombination radius, r_{rec} [nm]	0.65	0.65
Capture efficiency for vacancies by dislocations Z_v	1.0	1.0
Capture efficiency for interstitials by dislocations Z_i	1.2	1.2
Burgers vector of the loops assumed to be prismatic b [nm]	0.2	0.2
Pre-existing dislocation density ρ_0 [m^{-2}]	7.0×10^{13}	5.5×10^{13}
Average grain size d [m]	2.5×10^{-4}	1.0×10^{-6}

Cluster Dynamics Master Equation

Matrix defect system. The public domain library solver LSODA [3] has been used to integrate directly the master equation [4] for the study of the matrix defect subsystem containing free vacancies, spherical VC with sizes up to 1000 vacancies, free SIA (self-interstitial atoms) and planar SIAC with sizes up to 4000 SIA. The attachment coefficients for the master equation [4] are determined in the diffusion limited regime and following the approach reported in Ref. [5] for spherical VC and planar SIAC, respectively. The emission coefficients in Ref. [4] are fixed using the detailed balance principle for both, VC and SIAC. The values for the pre-existing dislocation density, ρ_0, and the average grain size, d, are taken from the experiment [1]. Other material parameters are found by fitting to the condition of best reproduction of the experimental data [1] by the results of the CD simulation. The final collection of material parameters used in present study are presented in the Table 1 in comparison to the data used in Ref. [4]. The only substantial change of material parameters with respect to Ref. [4] is the SIA diffusivity. The values of the pre-factor for SIA diffusion, D_{i0}, amounts to 4.8×10^{-8} m^2/s, and migration energy of the SIA, E_{mi}, is found at 0.24 eV in satisfying agreement with the simulation data [6] on the SIA diffusivity dependence on the Cr content in Fe-Cr alloys.

Cr precipitates system. The number density of the Cr precipitates, C_n, is determined from the master Eq. 1:

$$\frac{dC_n}{dt} = \beta_n \left(\left(\frac{n-1}{n} \right)^{1/3} C_{n-1} - \left(1 + \left(\frac{n-1}{n} \right)^{1/3} w_n \right) \cdot C_n + w_{n+1} \cdot C_{n+1} \right) \quad . \tag{1}$$

Here, n is the size of the Cr precipitate, $2 \leq n \leq N_{max}$, and C_n is set to zero for $n > N_{max}$, as is the case for all C_n at t = 0. β_n is the absorption rate of an n-atomic cluster as obtained in the diffusion limited regime:

$$\beta_n = 4\pi \sqrt[3]{\frac{3\Omega_{Cr}}{4\pi}} D_{Cr}^{irr} \frac{C_{1Cr}}{\Omega_{Fe}} n^{1/3} \quad , \tag{2}$$

where Ω_{Fe} and Ω_{Cr} are the atomic volume of bcc iron and bcc chromium, and C_{1Cr} is the concentration of the remaining solute chromium atoms in the matrix. For high chromium concentrations, size and concentration dependent correction factors for β_n have been proposed to account for the resulting overlapping diffusion field effects like the method discussed in Ref. [7]. Little impact on the precipitation is expected by such corrections despite a slight speed-up of the evolution [7]. The chromium concentration is determined via:

$$C_{1Cr} = C_{0Cr} - \sum_{n=2}^{N_{max}} n C_n \quad , \tag{3}$$

with C_{0Cr} being the initial concentration of the chromium atoms. D_{Cr}^{irr} is the irradiation enhanced diffusion coefficient of chromium in iron according to:

$$D_{Cr}^{irr} = D_{Cr}^{th} \frac{C_{1v}^{irr}}{C_{1v}^{eq}}, \tag{4}$$

where D_{Cr}^{th} is the thermal diffusion coefficient of chromium in iron calculated according to the Arrhenius law with the experimental parameters $D_0 = 1.29 \times 10^{-4} \, \text{m}^2/\text{s}$ and $E_m = 2.39 \, \text{eV}$ for Fe-12%Cr alloy [10]. C_{1v}^{eq} and C_{1v}^{irr} are the vacancy concentrations for the unirradiated and irradiated state of the material, respectively, with C_{1v}^{eq} being evaluated as in Ref. [4]. We focus on the vacancy exchange mechanism for the chromium mobility in the Fe-Cr system, because it is believed to be the dominant mechanism in the Fe-12.5%Cr alloy invested here (for more details see discussion). The emission parameter, w_n, finally, is calculated by the Eq. 5:

$$w_n = \exp\left(-\frac{\Delta\mu}{k_B T} \right) \exp \frac{4\pi\gamma^{cl,m} \left(R_n^2 - R_{n-1}^2 \right)}{k_B T} \quad , \tag{5}$$

where $\gamma^{cl,m}$ is the specific surface tension of the interface between the Cr cluster (cl) and the matrix (m), R_n is the radius of a Cr cluster of size n, k_B the Boltzmann constant, and $\Delta\mu$ is determined via

$$\Delta\mu = \left(\mu_{Cr}^m(C_{1Cr}) - \mu_{Cr}^{cl} \right) \cdot x_{Cr}^{cl} + \left(\mu_{Fe}^m(C_{1Cr}) - \mu_{Fe}^{cl} \right) \cdot x_{Fe}^{cl} \tag{6}$$

Here $\mu_{Cr}^{cl}\left(\mu_{Cr}^m\right)$ and $\mu_{Fe}^{cl}\left(\mu_{Fe}^m\right)$ are the chemical potentials of chromium and iron, respectively, in the precipitate cluster (matrix), and $x_{Cr(Fe)}^{cl}$ is the mole fraction of chromium (iron) in the Cr precipitate, which is set to 0.95 ± 0.05 according to the assumption of the equality of precipitate and matrix composition at the binodal miscibility curve.

Note, that no simple lattice gas (or ideal solution) behavior is imposed here to the dependence of the chemical potential in the matrix on the Cr concentration. Instead the chemical potential of chromium (iron) in both subsystems, matrix and precipitate, is taken from Eq. 7:

$$\mu_{\text{Cr(Fe)}} = \frac{\partial}{\partial n_{\text{Cr(Fe)}}}\left((n_{Cr} + n_{Fe})\frac{G}{N_{\text{A}}}\right) \quad , \tag{7}$$

where n_{Cr} (n_{Fe}) is the number of chromium (iron) atoms in the respective Fe-Cr subsystem, N_{A} is the Avogadro number, and G is the total *molar* Gibbs free energy as obtained from the expression used by CALPHAD [11]:

$$G = x_{\text{Cr}}G_{\text{Cr}}^{\text{bcc}} + x_{\text{Fe}}G_{\text{Fe}}^{\text{bcc}} + RT(x_{\text{Cr}}\ln x_{\text{Cr}} + x_{\text{Fe}}\ln x_{\text{Fe}}) + G_{\text{ex}}^{\text{bcc}} + G_{\text{M}}^{\text{bcc}} \tag{8}$$

Here R is the gas constant, $x_{\text{Cr}}(x_{Fe})$ is the chromium (iron) mole fraction – or equivalently, the concentration measured in atoms per site – in the respective Fe-Cr subsystem. $G_{\text{Cr}}^{\text{bcc}}(G_{\text{Fe}}^{\text{bcc}})$ is the molar free energy of pure bcc Cr(Fe) as reported in [12], and $G_{\text{M}}^{\text{bcc}}$ is the magnetic contribution to the molar excess free energy proposed by [13]. A regular solution model is used in [11] for the non-magnetic molar excess free energy $G_{\text{ex}}^{\text{bcc}}$ in the Fe-Cr system. This expression has been modified by G. Bonny [14] in order to account for the recently proposed modification of the Fe-rich phase boundary [15] for temperature well below 800 K. We found that the Redlich-Kister polynomial given in Ref. [14] could equally well be written in following factorized form:

$$G_{\text{ex}}^{\text{bcc}} = x_{\text{Cr}}(1 - x_{\text{Cr}}) \cdot \left[20500 - 9.68 \cdot T + L(x_{\text{Cr}}) \cdot \left(1 - \frac{T}{1100}\right)^3 \theta\left(1 - \frac{T}{1100}\right)\right] \text{ J/mol}, \tag{9}$$

where

$$L(x_{\text{Cr}}) = 8615.407399 + 431.3047159(2x_{\text{Cr}} - 1) - 31452.7845(2x_{\text{Cr}} - 1)^2 +$$
$$48134.04065(2x_{\text{Cr}} - 1)^3 - 23569.11288(2x_{\text{Cr}} - 1)^4 - 5625.73983(2x_{\text{Cr}} - 1)^5 \tag{10}$$

and $\theta(x)$ is the Heavyside function being one for $x \geq 0$ and zero else. All coefficients in Eqs. 9 and 10 are given in SI units (i.e., in J/mol and K). Relating the ratio w_{n} between the absorption and emission rates entering Eq. (1) to chemical potential differences and deriving these differences from empirical thermodynamic free energy expressions is an empirical way to account for the so-called frustration effects due to higher solute atom and/or cluster concentrations in the system as discussed in Refs. [8,9]. Again the library solver LSODA has been used to integrate the master equations (1-6) in order to find the precipitate cluster concentrations C_n for all n up to $N_{\text{max}} = 9000$.

Cluster dynamics modelling

The results from the CD modelling on the dose dependence of the free vacancy and SIA concentrations, C_{1v}^{irr} and C_{1i}^{irr}, the mean radius of the VC and mean diameter of the SIAC, $(R_{\text{v}})_{\text{mean}}$ and $(2R_{\text{i}})_{\text{mean}}$, the total number density of SIAC, N_{i}, the volume fraction of the Cr precipitates, $C_{\text{v,Cr}}$, and the mean radius of the Cr precipitates, $(R_{\text{Cr}})_{\text{mean}}$, are shown in the Figures (1-4).

It was found that the CD simulation according to the procedure used in Ref. [4] but with taking into account the chromium effect on the SIA diffusivity reported in [6] allows to reproduce the experimental TEM data [1] on N_{i} exactly (Fig. 1) and on $(2R_{\text{i}})_{\text{mean}}$ approximately (Fig. 2). A saturation behavior under neutron irradiation is observed for both, C_{1i} and N_{i}, at doses higher than about 0.006 dpa (Fig. 1). The loop diameters $(2R_{\text{i}})_{\text{mean}}$ found in the simulations increase slowly with neutron irradiation and reach 5.74 and 6.25 nm for the neutron doses of 0.6 and 1.5 dpa, respectively (Fig. 2), instead of about 6 nm for both doses as observed experimentally [1].

A value of about 1.73×10^{21} m^{-3} is found in the CD simulation for the number density of the SIAC at the experimental neutron doses of 0.6 and 1.5 dpa. The same value was observed by TEM [1]. According to our CD simulations no change in N_i is expected for any neutron doses between 0.006 dpa and 12 dpa. The strong peak in the SIAC distribution at diameters of about 0.5 nm (see Fig. 3) is observed for all neutron exposures. The value of $(R_v)_{mean}$ increases only slowly up to an irradiation dose of about 6×10^{-4} dpa. Then it increases faster but does never exceed 0.5 nm (Fig. 2), which is the experimental resolution limit of both SANS and TEM techniques. Thus our finding is in line with the fact, that no VC has been detected in the experimental studies [1, 2].

The Cr precipitates evolution was found to be rather sensitive to the surface tension $\gamma^{cl,m}$ of the interface between the precipitate cluster and the α matrix. Using 0.218 J/m^2, 0.155 J/m^2, and 0.048 J/m^2 as $\gamma^{cl,m}$ values for the coherent interfaces [100], [111] and [110] reported in Ref. [16] does not allow to reproduce the SANS data [2]. A value for $\gamma^{cl,m}$ of about 0.028 J/m^2 is necessary to approximately reproduction the SANS data [2] on the dose dependence of the volume fraction $C_{v,Cr}$ and the mean radius (R_{Cr})$_{mean}$ of the Cr-rich α' precipitates by the CD simulations (Fig. 4). The saturation of the simulated $C_{v,Cr}$ values at about 4.0 vol% is observed for the same neutron exposes as the saturation of the N_i values.

Discussion

The CD model used in this study is close to the CD-P-VIC model from Ref. [17], where the CD simulations are first performed for the free vacancies, SIA and point defect clusters and then for the precipitates taking into account the actual time dependence of the free point defect concentrations obtained in the first step. In additional to Ref. [17] we take into account the Cr-effect on the SIA diffusivity according to the DFT calculations reported in Ref. [6]. By fitting the parameters governing the behavior of the SIA in the matrix satisfying agreement of the CD simulation data with the experimental TEM data [1] could be achieved.

The assumptions used to study the evolution of the Cr precipitates need special attention. Two different mechanisms are discussed in Ref. [18] for the irradiation induced or enhanced formation of α' precipitates in Fe-Cr alloys. The first mechanism suggested for the migration of Cr to the voids is the exchange of chromium atoms with vacancies [18]. This statement is in line with DFT calculations predict a relatively low barrier for chromium atom exchange with a vacancy in iron [19]. As a second mechanism proposed, relies on the strong interaction between chromium atoms and SIA leading to a transport of Cr atoms to SIA loops. However, the latter mechanism is not supported by the TEM data [1], where decorated dislocation loops are only observed in the irradiated Fe-9at%Cr alloys but not for the Fe-12.5at%Cr alloys. That is, why we focus on the vacancy exchange mechanism in Eq. (4).

A more complete study of Cr precipitation by CD should include the formation and migration of Fe-Cr interstitial as additional link between the CD master equations for the self-defects and the CD master equations for the Cr precipitates. Yet, the diffusion of single chromium atoms, contrary to SIA and vacancies, towards the dislocation net and the irradiation induced VC and SIAC is not considered. This is done, because the diffusivity of chromium is about ten orders of magnitude lower than the diffusivity of vacancies and SIA at a temperature of 573 K, and the strength of any sink is proportional to the diffusivity of the trapped species.

Another assumption is the applicability of the usual CD formalism [20] to study the evolution of Cr-precipitates in a binary alloy with concentrations as high as in Fe-12.5%Cr. Treating the Cr absorption in Fe-12.5at%Cr like in a dilute lattice gas is only correct approximately. There are ways to account for the overlapping diffusion field effects in more concentrated alloys, but they have not

been considered in the present study. Little impact, despite a slight overall speed-up of the Cr precipitation process is expected from such corrections [7]. In addition, frustrations effects are likely to occur in concentrated alloys [8,9] leading to a non-linear dependence of the ration w_n between the absorption and emission rates of the precipitate clusters. This effect has been taken into account empirically by the use of the thermodynamic free energy expression from CALPHAD [11] wit the correction suggested by Bonny et al. [14]. Moreover, the size distribution function of the Cr precipitates [2] which is used for calibration in our study, has been derived (as suggested in Ref. [22]) from SANS data in a Q-range, where the interference effect for concentrated alloy does not occur.

In order to quantify the amount to which the Fe-12.5at%Cr alloy deviates from an ideal lattice gas, we follow the approach suggested in Ref. [9,21] and estimate the fraction of the exclusion volume from the SANS data [2]. To this end, the interference factors $S(Q)$ is determined for Q-range, where the interference effect is observed. Then the mono-disperse hard-sphere model [23] which takes into account the correlation between all hard spheres, is applied to interpret the obtained interference factor. The volume fraction of the hard spheres is found at 14.4% and 13.3% for the irradiation doses of 0.6 and 1.5 dpa, respectively. These values seem to be upper limits for the fraction of the exclusion volume according to Ref. [9]

There is indeed some deviation in the Cr precipitation process from the ideal lattice gas behavior, and although the most dominant frustration effect has been accounted for empirically, it could easily be that some of the drawbacks of not treating the frustration effect more rigorously and not considering other effects, like the overlapping diffusion field effect on the absorption rate is compensated by the low fit value of surface tension $\gamma^{cl,m}$ in our CD model, as compared to the DFT data given in Ref. [16]. Nevertheless, applying our CD formalism is a reasonable first approximation to the investigation of the long-term evolution of chromium precipitates in Fe-Cr alloys of moderate concentrations around 12.5 at%.

Summary

Cluster dynamic (CD) simulations according to Ref. [4], including the effect of the chromium concentration on the SIA diffusivity [6], are able to the reproduce the experimental TEM data [1] on the SIAC size distribution satisfactorily. A saturation behavior of the total number density of SIAC in neutron irradiated Fe-12.5at%Cr model alloys for neutron expose in the range from 0.006 dpa to 12 dpa is predicted. The CD simulations also indicate the presence of VC with radii less than 0.5 nm and a strong SIAC peak with a mean diameter of about 0.5 nm, both invisible in SANS and TEM experiments because of the resolution limits of these techniques.

By adjusting the surface tension between the α matrix and the α' precipitates it was possible to reproduce the SANS data [2] on the long-term behavior of the Cr precipitates. The resulting specific interface energy of 0.028 J/m^2 is noticeably lower than expected from DFT calculations [16]. Using the more rigorous approach to the frustration effect on the emission rates suggested in Ref. [9,21], considering the overlapping diffusion field effect in the absorption rates (as in Ref. [7] for instance) and taking into account the formation and migration of Fe-Cr interstitial as additional link between the CD master equations for the self-defects and the CD master equations for the Cr precipitates, may lead to somewhat higher value of the surface tension.

Acknowledgment

References

[1]   M. Matijasevic, A. Almazouzi, Journal of Nuclear Matererals, Vol. 377 (2008), p.147

[2]   F. Bergner, A.Ulbricht, C. Heintze, Scripta Materialia, Vol. 61 (2009), p.1060

[3]   LSODA is part of the ODEPACK provided by Alan C. Hindmarsh on the CASC server of the Lawrence Livermore National Laboratory, Livermore, CA 94551, U.S.A.

[4]   A. Gokhman, F. Bergner: Radiation Effects and Defects in Solids, Vol. 165 (2010), p.216

[5]   A. Hardouin Duparc, C. Moingeon, N.Smetaninsky-de-Grande, A.Barbu, Journal of. Nuclear Materials, Vol. 302 (2002), p.143

[6]   D. Terentyev, P. Olsson, T.P.C. Klaver, L. Malerba, Computational Materials Science, Vol. 43 (2008), p. 1183

[7]   E. Clouet, A. Barbu, L. Laé, and G. Martin, Acta Materialia **53** (2005) 2313-2325.

[8]   J. Lepinoux, Acta Materialia **57** (2009) 1086-1094.

[9]   J. Lepinoux, Philosophical Magazine Vol. 86 (2006), p.5053

[10]   R.A.Wolfe, H.W. Paxton, "Diffusion in BCC metals", Transactions of the metallurgical Society of AIME, Vol. 230 (1964), p.1426

[11]   J.-O. Andersson, B. Sundman, CALPHAD 11 (1987) 83.

[12]   A.T. Dinsdale, CALPHAD 15 (1991) 317.

[13]   M. Hillbert, M. Jarl, CALPHAD 2 (1978) 227.

[14]   G. Bonny, PhD thesis, Universiteit Gent, 2009, ISBN 978-90-8578-296-4.

[15]   G.Bonny, D.Terentyev, L.Malerba, Scripta. Materialia, Vol. 59 (2008), p.1193

[16]   Duc Nguyen-Manh, M. Yu. Lavrentiev, S.L. Dudarev, C.R. Physique Vol. 9 (2008), p.379

[17]   F. Christien, A. Barbu, Journal of Nuclear Materials, Vol. 324 (2004), p. 90

[18]   L. Malerba, A. Caro, J. Wallenius, Journal of Nuclear Matererals, Vol. 382 (2008), p.112

[19]   P. Olsson, C. Domain, J. Wallenius, Phys. Rev. B75 (2007) 014110

[20]   G. Martin, Advanced Engineering Materials Vol. 8 (2006), p. 1231

[21]   J. Lepinoux, Philosophical Magazine Vol. 90 (2010), p. 3261

[22]   P. Staron, PhD thesis, Universität Hamburg, 1997, also published as Report GKSS 97/E/53, GKSS Forshungszentrum Geesthacht, 1997

[23]   D. J. Kinning, E.L. Thomas, Macromolecules Vol. 17 (1984), p.1712

Figures
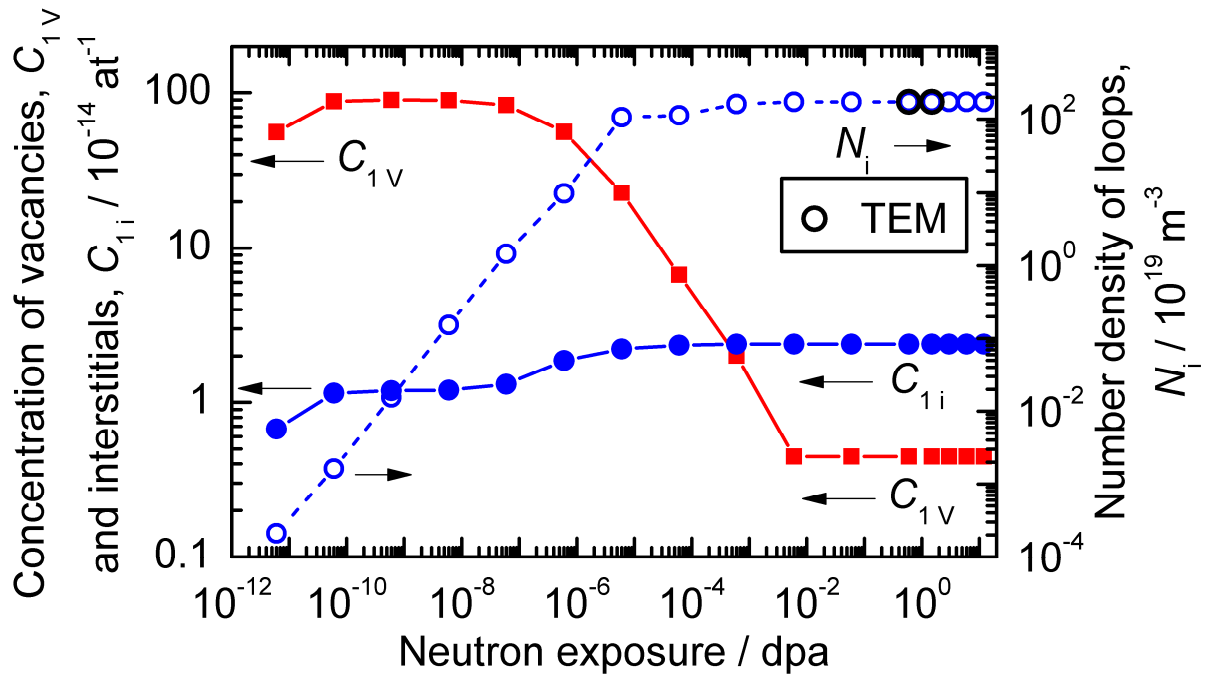

Fig. 1. Dose dependence of the free vacancy (SIA) concentrations, C_{1v}^{irr} (C_{1i}^{irr}), and the total number density of SIAC, N_i, for the irradiated Fe-12.5at%Cr alloy according to the TEM experiment [2] and the CD simulations.
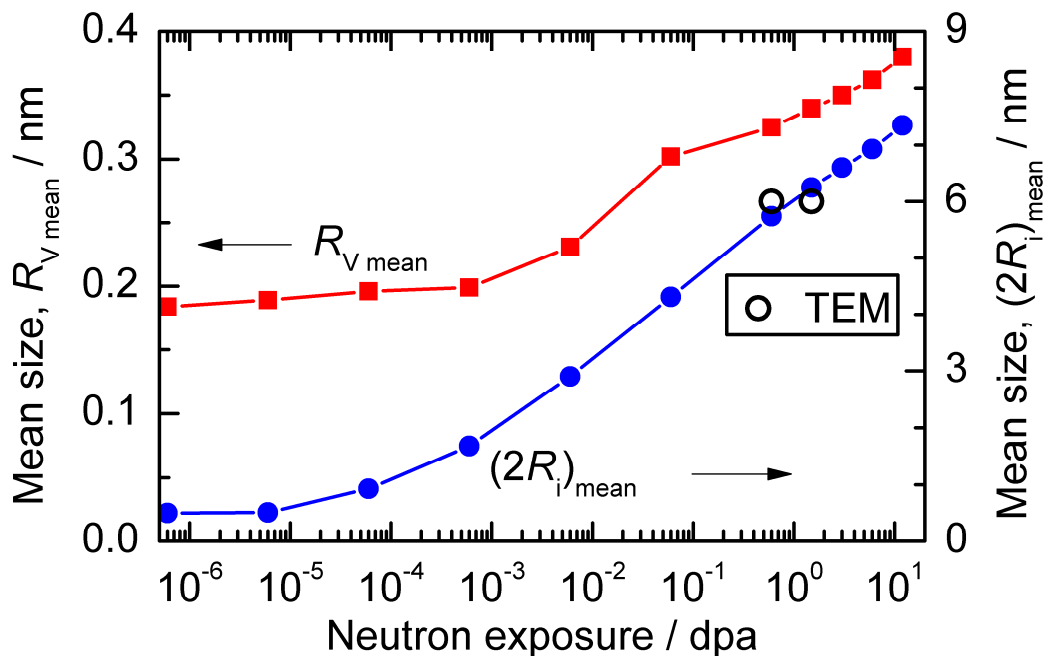
Fig. 2. Dose dependence of the mean radius of the VC and the mean diameter of the SIAC, $(R_v)_{mean}$ and $(2R_i)_{mean}$, for the irradiated Fe-12.5 at%Cr alloy according to the TEM experiment [2] and the CD simulations.
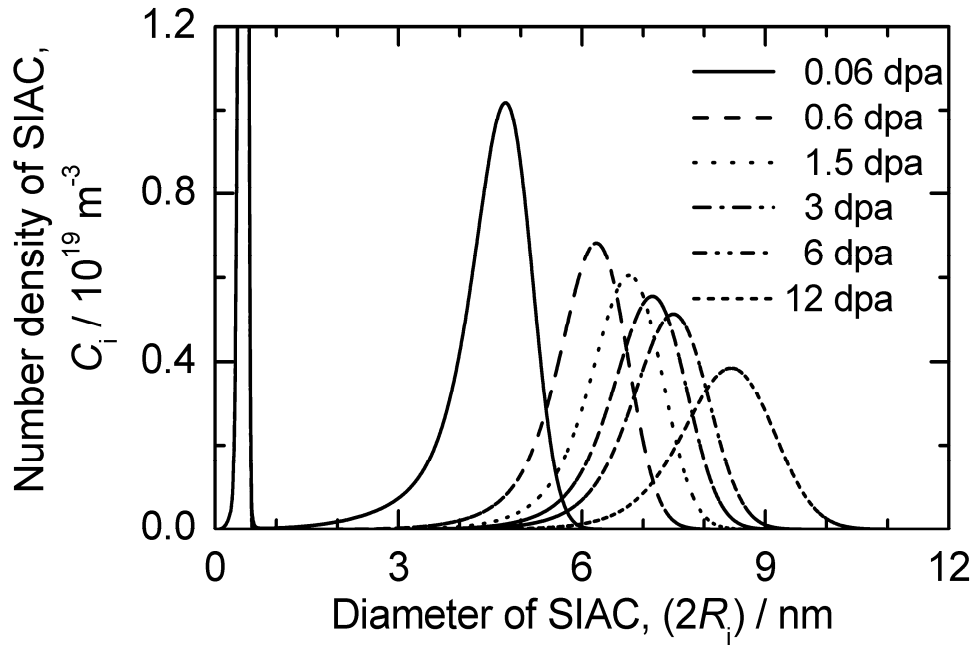
Fig. 3. Size distributions of self interstitial atom cluster in Fe-12.5%Cr for different irradiation conditions as obtained from the CD simulations.
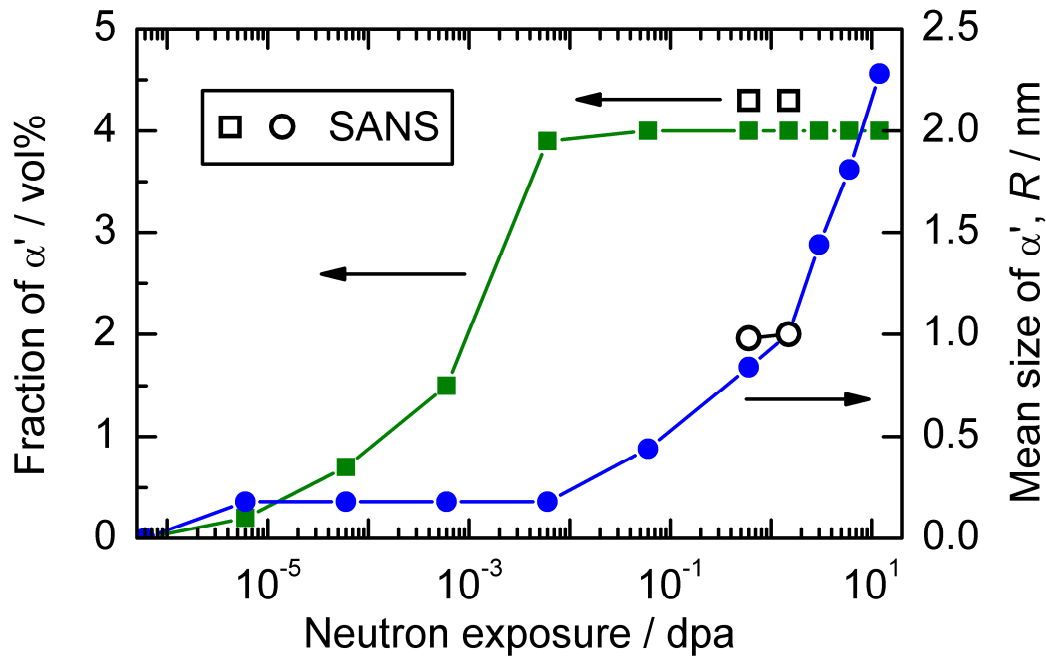
Fig. 4. Dose dependence of the volume fraction and mean radius of the Cr precipitates, $C_{v,Cr}$ and $(R_{Cr})_{mean,}$ for the irradiated Fe-12.5%Cr alloy according to the TEM experiment [2] and the CD simulations.

Solid-Solid Phase Transformations in Inorganic Materials

Cluster Dynamics Study of Neutron Irradiation Induced Defects in Fe-12.5at%Cr Alloy